Int. J. Electrochem. Sci., 12 **(2017)** 485 – 495, doi: 10.20964/2017.01.48

International Journal of
ELECTROCHEMICAL
SCIENCE
www.electrochemsci.org

Study on Electrochemistry and Nucleation Process of Nickel Electrodeposition

Yundan Yu, Lixia Sun[*]*, Hongliang Ge, Guoying Wei, Li Jiang*

College of Materials Science and Engineering, China Jiliang University, China
[*]E-mail: lixiasun1982@sina.com

Received: 16 October 2016 / *Accepted:* 17 November 2016 / *Published:* 12 December 2016

Nickel thin films were prepared by plating technology on glassy carbon to investigate electrodeposition mechanism and nucleation process. Princeton parstat 2273 station was used to analyze nickel electrodeposition process based on cyclic voltammetry, polarization curves, chronoamperometry and so on. According to the cyclic voltammetry, cathode current and deposition mass of nickel increased extremely when the voltage was more negative than -1.0 $V_{SCE.}$ Higher sweeping voltage would lead to stronger cathodic polarization and more deposition mass. Cyclic voltammetry curves with different scan rates indicated that nickel deposition was a kind of irreversible and electrochemistry-limited process. Regarding to typical nucleation model promoted by Scharifker and Hills, the results obtained from chronoamperometry curves with different deposition voltages showed that nickel electrodeposition on glassy carbon was a kind of three dimensional models with progressive nucleation process. Nickel deposition were a kind of grain films with typical bulk structures because three dimensional progressive nucleation mechanism.

Keywords: nickel films; electrochemistry mechanism; progressive nucleation;

1. INTRODUCTION

With the development of microelectromechanical systems, smaller size magnets are required as components. Magnet films play a big role in the microelectromechanical system, which could be widely used in micro-driver, micro-sensor, energy collector and so on. Nickel possesses high melting point, high hardness and better mechanical properties. It is found out that nickel alloys have the advantage of compact structure and excellent corrosion resistance. Moreover, nickel alloy films have optimal magnetic performance, not only can be used as a high density perpendicular magnetic recording medium, but also could instead of tiny magnets in the microelectromechanical system.[1-5]

Many works have been reported about optimal properties of nickel based alloy films. For example, structural and magnetic properties of nickel alloys ferrites synthesized by coprecipitation method were investigated by Shaikh.[6] Campos reported an investigation of thin Ni and nickel alloys electrodeposited over flexible substrates.[7] Sun fabricated a kind of nickel alloys permanent magnet arrays for sensors and actuators.[8] Electrochemical deposition of CoNi as new materials for electrochemical sensing of glucose was studied by Vilana.[9] There are many methods that could be used to prepare nickel alloy films, such as plating, physical vapor deposition, molecular beam expitaxy and so on. Each approach contains its advantages and disadvantages. However, considering about economy and convenience, plating technology is a kind of very effective and efficient ways to prepare alloy films which do not need too much equipment, but offer highly selective and conformal coatings.

Some works have been reported so far about preparing nickel alloy films by electrodeposition methods. For instance, J.Vazquez-Arenas investigated surface texture properties of CoNi alloys obtained by plating.[10] Ni-TiN thin films were electrodeposited by Fafeng Xia.[11] A kind of nanocomposite coatings based on NiW alloys were obtained by Wasekar[12] In addition, Zakeri prepared (Zn-Ni)/nano Al_2O_3 composite coatings by plating technology.[13] Nickel based alloy films have been becoming the hot spot of functional films. Therefore, nickel based alloy films prepared by plating technology have been studied extensively.[14-18] However, it is found out that plating technology also possesses some disadvantages, such as particles aggregation, rough surface, concentration polarization, hydrogen evolution and so on. Along with the rapid development of electromagnetic technology, magnetic plating technology has gained much more focus which could ameliorate the problems during electrodeposition process. Magnetic field induced during electrodeposition process to prepare alloy thin films is called magnetic plating technology which could effectively improve deposition rate, refine coatings, reduce concentration polarization and so on. Nickel and cobalt are typical elements with ferromagnetic properties. The effect of magnetic field on cobalt and nickel during plating process is conspicuous. Detail work about influences of magnetic fields on cobalt and cobalt alloys during plating process was investigated by our group.[16-17] According to our research, effects of magnetic fields on plating process with different electrochemistry and nucleation mechanism was totally different. Specific information about electrochemistry mechanism for cobalt electrodeposition process was reported in detail in our previous work. [19] However, basic electrodeposition mechanism of nickel is seldom reported in detail. Understanding electrodeposition mechanism of nickel is significant to comprehend deposition mechanism of nickel based alloys. Therefore, some basic research was done in the paper to investigate electrochemistry and nucleation process of nickel based on cyclic voltammetry, impedance, polarization curve, transient curves and so on.

2. EXPERIMENTAL PART

The electrodeposition system of nickel was based on three electrodes. Glass carbon discs with 0.5 cm and 1 cm diameter were chosen as working and counter electrodes respectively. Saturated Calomel electrode (SCE) was designed as reference electrode. The plating solution was composed of

0.1 M NaCl and 0.01 M $NiCl_2$ without any chemical additives. Fig.1 below showed chart of nickel plating process.

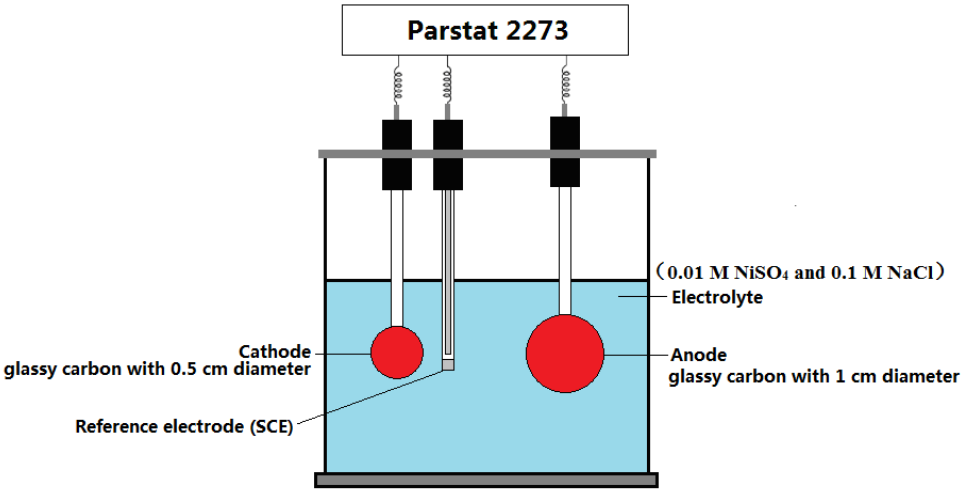

Figure 1. Chart of nickel electrodeposition process

According to Fig.1, $NiCl_2$ and NaCl were used as source of nickel and conducting salt respectively. Working pH was up to 4.0 and the working temperature was 25 ℃. A polish machine (MP-1A) was utilized to polish the surface of glassy carbon before the experiment to make the date more precisely. At last, the glassy carbon was immerged into 100 ml electrolyte to perform electrodeposition. Princeton parstat 2273 station was used to research electrochemical process of nickel based on cyclic voltammetry method, AC impedance, and transient state analysis. Moreover, quartzmicrobalance (QCM25) was utilized to monitor the deposition mass on cathode. It is known that the quartzmicrobalance possesses extremely sensitive sensors which are capable of measuring mass changes in μg/cm^2. Sauerbrey equation was used in the paper to calculate the mass changes during cobalt electrodeposition process.

$$\Delta f = -C_f \Delta m \qquad \text{Equation (1)}$$

Where, Δf is the observed frequency change in Hz, Δm is the change in mass per unit area (μg /cm2), and C_f is the sensitivity factor for crystal (56.6 Hz cm^2/μg).

3. RESULTS AND DISCUSSION

3.1 Electrochemical process of nickel electrodeposition

Quartzmicrobalance were used to monitor mass of nickel deposited on cathode. According to Fig.2, cathode current and mass changing were basically equal to zero when the sweeping voltage increased from 0 to -0.2 V_{SCE} (position a). It stated that there was no nickel deposition from 0 to -0.2 V_{SCE}. However, cathode current and mass changing started to increase with the sweeping voltages

ranged from -0.2 V_{SCE} (position a) to -1.0 V_{SCE} (position c). According to Fig.2(b), mass of nickel increased slowly from a' to c' which meant that hydrogen evolution was dominated at this range. Cathode current and deposition mass of nickel increased extremely with the sweeping voltage ranged from -1.0 V_{SCE} (position c) to -1.5 V_{SCE} (position d). Higher sweeping voltage would lead to stronger cathodic polarization process and more deposition mass. Moreover, there was no obvious reduction peak could be detected from position c to d. This phenomenon could determine that nickel deposition process basically belonged to electrochemical controlling mechanism. However, cobalt electrochemsitry deposition process was different from nickel. Cobalt deposition associated with hydrogen evolution started at −0.3 V_{SCE} while cobalt deposition was dominated at −1.1 V_{SCE}. With the increase in scan rate, potential of cobalt deposition shifted more negative. Values of reduction and oxidization peaks were unsymmetrical especially at lower scan rate which indicated that the reduction of cobalt on glassy carbon surface was an irreversible process.[19-21]

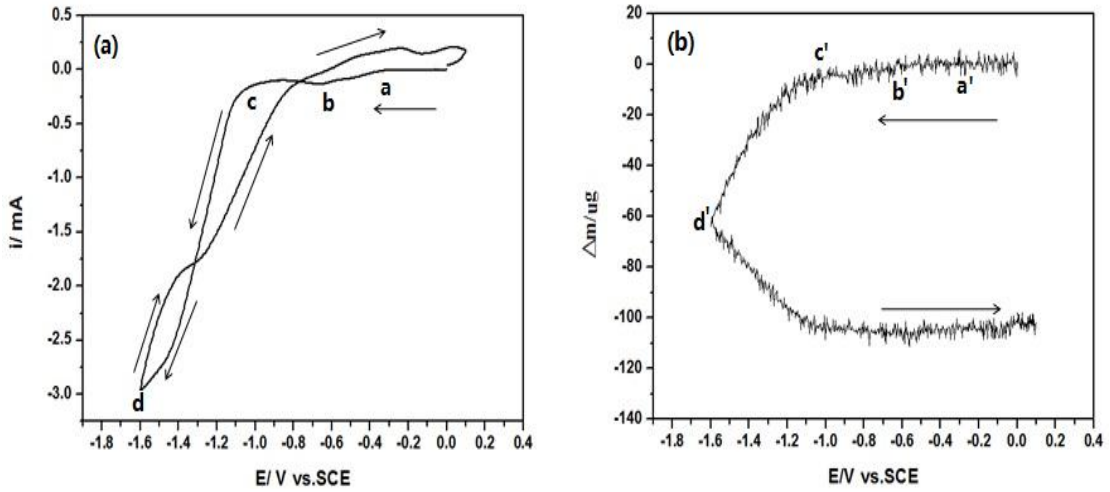

Figure 2. cyclic voltammogram of nickel plating process (working electrode: 1.37 cm^2 Au disc of QCM; counter electrode: glass carbon; reference electrode: SCE ; 0.01 M $NiSO_4$+0.1 M NaCl with scan rate 10 mv/s;)

Electrochemical reaction on the surface of electrode during electrodeposition process is considered as two kinds of limiting mechanisms: electrochemistry and diffusion controlling. If the diffusion rate of species is faster than reaction rate in the plating system, the electrodeposition system is controlled by electrochemistry reaction. However, during the plating process, if diffusion rate of species is slower than reaction rate, the electrodeposition system is controlled by diffusion. Understanding the limiting mechanism of nickel deposition is very significant and important for studying nucleation and electrochemistry process. Therefore, cyclic voltammetry curves with various scan rates ranged from 5 to 50 mv were utilized to investigate the mechanism of nickel plating, which was shown in Fig.3.

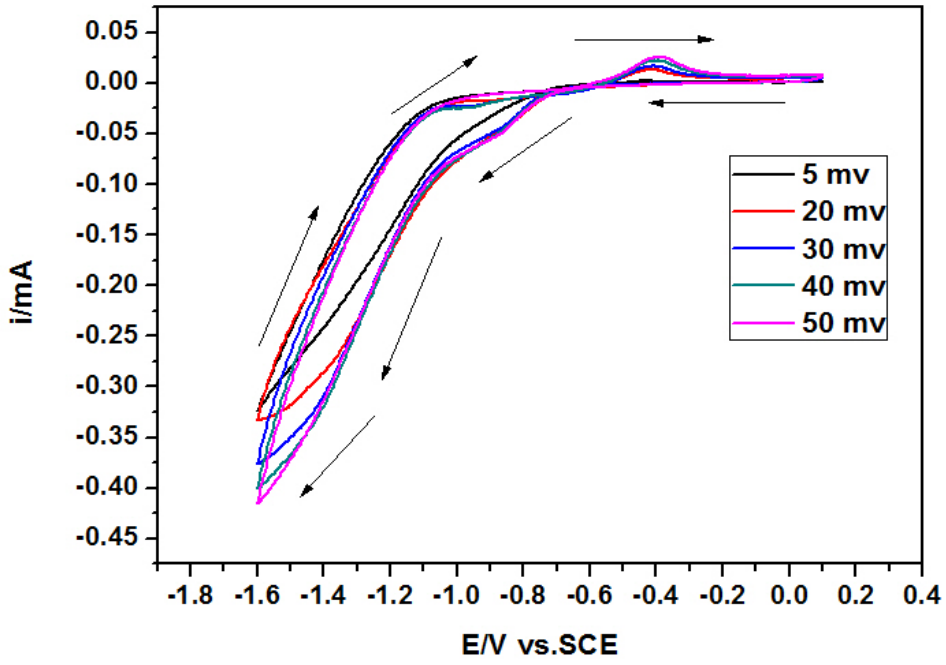

Figure 3. Nickel cyclic voltammetry curves with different scan rates (working electrode: 0.5 cm diameter glass carbon; counter electrode: 1 cm diameter glass carbon; reference electrode: SCE; 0.01 M $NiSO_4$+0.1 M NaCl)

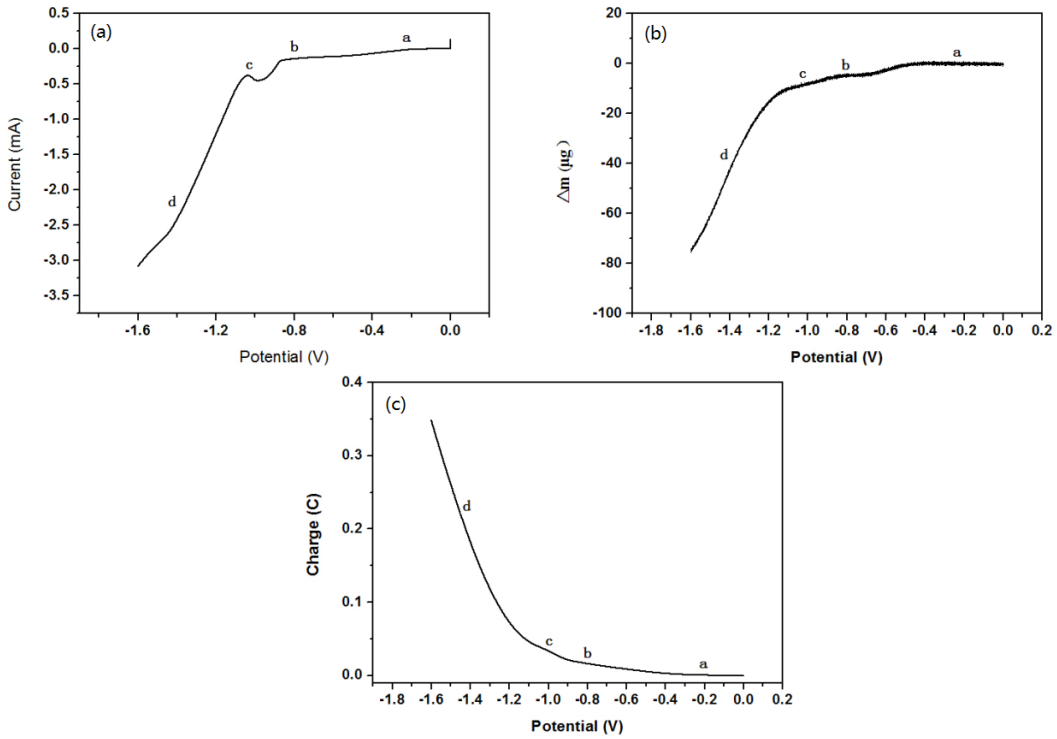

Figure 4. Polarization curves of nickel electrodeposition process (working electrode: 1.37 cm^2 Au disc of QCM; counter electrode: glass carbon; reference electrode: SCE ; 0.01 M $NiSO_4$+0.1 M NaCl with scan rate 10 mv/s)

Regarding to Fig.3, nickel deposition associated with hydrogen evolution started at -0.2 V_{SCE} while nickel deposition was dominated from about -1.0 V_{SCE}. With the sweeping voltage moving more negative than -1.0 V_{SCE}, cathodic current increased gradually. The faster scanning rate, the larger the cathodic current could be observed. Moreover, according to the cyclic voltammetry curves, no obvious nickel reduction peaks were observed under different scan rates, which stated a typical electrochemical controlling process. Consequently, regarding to the results drawn from above, it was found out that nickel deposition on glass carbon was a kind of typical electrochemical controlling process. However, cobalt deposition on glass carbon was a kind of typical diffusion controlling process.[22-24]

It was possible to calculate current efficiency of nickel at each stage of electrodeposition process based on polarization curve combined with QCM system. Detail information was shown in Fig.4 and Table 1.

Regarding to Fig.4, nickel deposition mass increased slowly combined with hydrogen evolution from position a to b. It was known that hydrogen evolution was dominated at the interval from a to b. The current efficiency was about 14.3% between the position a and b. However, nickel deposition was predominated at the interval from position b to d which possessed the current efficiency of 58.8%. According to the conclusion drawn from others, current efficiency of cobalt at the same condition was higher than nickel. [19]

Table 1. Electrochemistry parameters of nickel electrodeposition

Position	Voltage（V_{SCE}）	Current（μA）	Time（S）	Charge（mC）	Theoretical Deposition Mass (μg)	Actual Deposition Mass (μg)	Current Efficiency
a	-0.182	-4.74	19.3	2.272	-	-	-
b	-0.7944	-137.4	79.4	28.18	8.53	1.22	14.3%
c	-1.101	-1230.1	108	40.45	12.29	5.73	46.6%
d	-1.39	-2355.4	139	177.18	53.89	31.7	58.8%

3.2 Nucleation mechanism of nickel electrodeposition process

Chronoamperometry curves of nickel electrodeposition process with different deposition voltages ranged from -1.0 V_{SCE} to -1.4 V_{SCE} were investigated to study nickel nucleation mechanism.

Chronoamperometry curves of nickel electrodeposition with different voltages were approximately the same. At the short beginning of nickel electrodeposition process, the electric double layer was charged resulting in decrease of cathodic current. Along with the nickel ions diffused to the cathode surface and get electrons, cathode current started to increase and reach the peak. Subsequently, the cathode current started to decrease with the rise on thickness of diffusion layer. After the system reached an equilibrium state, the current density maintained a constant value. This phenomenon verified that nickel electrodeposition on glassy surface exhibited a typical three-dimensional nucleation process.

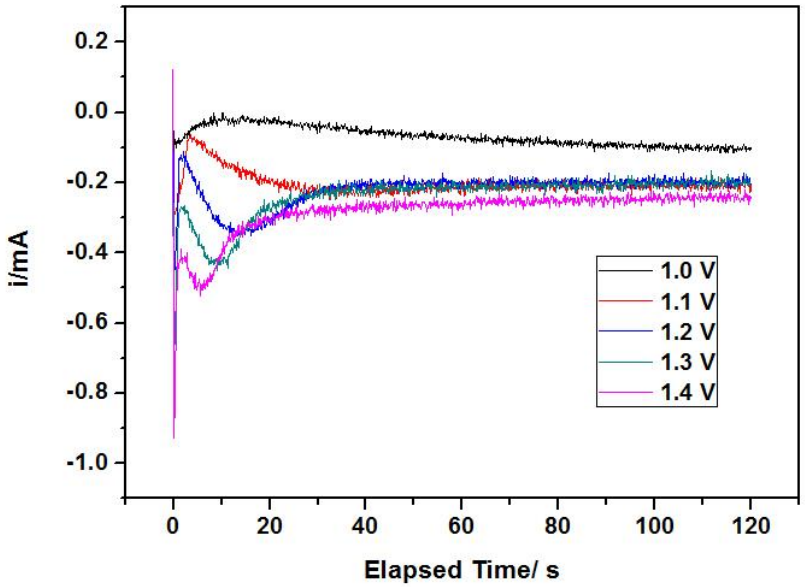

Figure 5. Chronoamperometry curve of nickel electrodeposition process (working electrode: 0.5 cm diameter glass carbon; counter electrode: 1 cm diameter glass carbon; reference electrode: SCE; 0.01 M $NiSO_4$+0.1 M NaCl;)

This conclusion is same to cobalt electrodeposition nucleation process reported by our group.[19] There were three important electrochemistry parameters based on chronoamperometry curves: peak current (i_m), time taken to get peak current (t_m) and equilibrium current (i_L). Especially, i_m and t_m were very important to study metal nucleation process at the early stage of electrodeposition process. Instantaneous nucleation and progressive nucleation were two kinds of typical nucleation models. Metal nucleation rate could be expressed as:

$$\frac{dN}{dt} = A(N_0 - N) \qquad \text{Equation (2)}$$

where, N stands for Number of crystal nucleus density (cm^{-2}), N_o is number of active position, A is nucleation rate constant (s^{-1});

For progressive nucleation model, At<1, so

$$N = AN_0 t \text{ and } \frac{dN}{dt} = AN_0 \qquad \text{Equation (3)}$$

For instantaneous nucleation model, At>1, so

$$N = N_0 \text{ and } \frac{dN}{dt} = 0 \qquad \text{Equation (4)}$$

From the equations above, it was clear that instantaneous nucleation had nothing to do with time, but had relationship with number of active position. However, progressive nucleation model had something to do with rate constant.

The traditional method used to confirm the nucleation model was determined by Scharifker and Hills. Equations about instantaneous and progressive nucleation model were described below:[25]

Instantaneous Nucleation: $\frac{i^2(t)}{i^2{}_{\max}} = \frac{1.9542}{t/t_{\max}}\left\{1-\exp\left[-1.2564(\frac{t}{t_{\max}})\right]\right\}^2$ Equation (5)

Progressive Nucleation: $\frac{i^2(t)}{i^2{}_{\max}} = \frac{1.2254}{t/t_{\max}}\left\{1-\exp\left[-2.3367(\frac{t}{t_{\max}})\right]\right\}^2$ Equation (6)

Where the i_{max} and t_{max} are the maximum peak current in the chronoamperometric diagrams and the time taken to get the peak current. The data obtained from the chronoamperometry curves could be expressed in the form of $(i/i_{max})^2$ against (t/t_{max}). These results were compared to the theoretical nucleation model to determine the nucleation type. The relationship between $(i/i_{max})^2$ and (t/t_{max}) was shown in Fig.6.

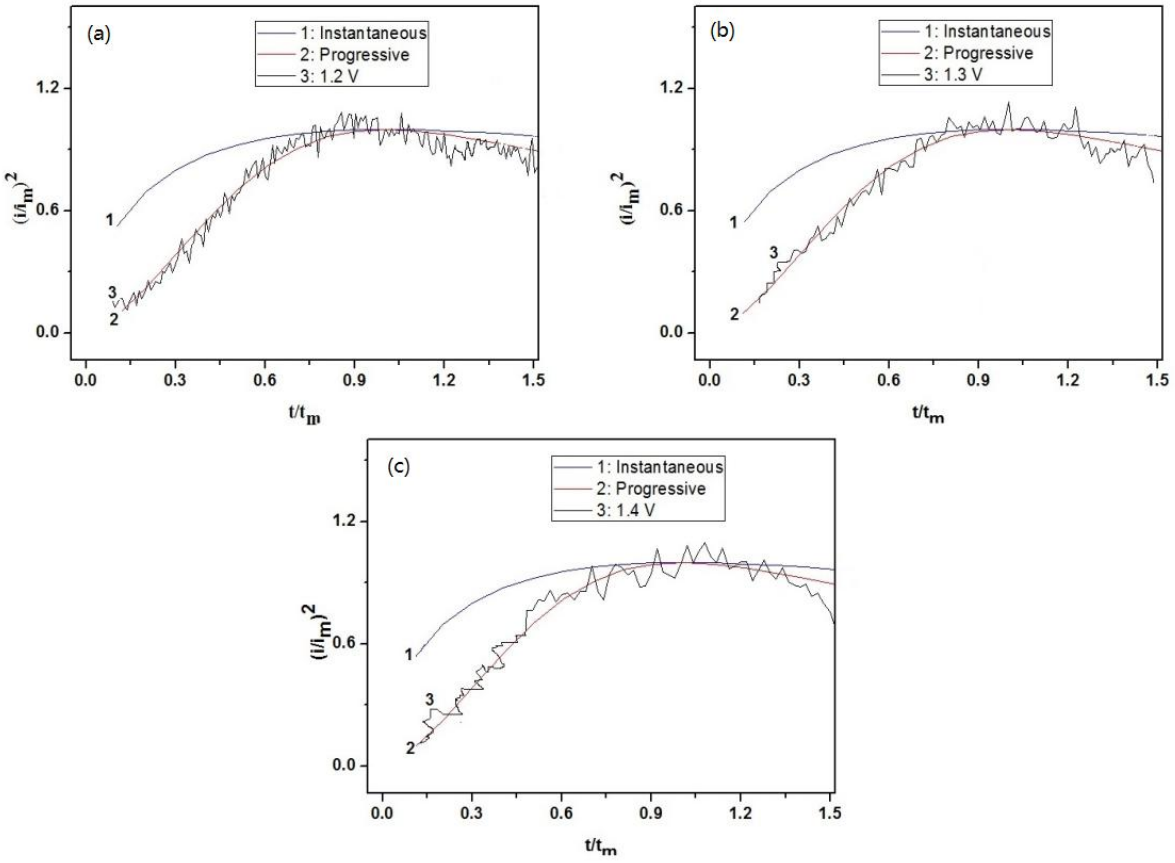

Figure 6. The experimental and theoretical plots of $(i/i_{max})^2$ against (t/t_{max}) from different chronoamperometry curves.

Regarding to Fig.6, sign 1 standed for instantaneous nucleation while sign 2 indicated progressive nucleation. It was very obvious that nickel electrodeposition on glassy carbon was a kind of typical progressive nucleation process. Therefore, from the results obtained from above, nickel electrodeposition on glassy carbon belonged to three dimension progressive nucleation mechanism. However, cobalt electrodeposition process was different from nickel which belonged to instantaneous nucleation mechanism. Some reports have been done about nucleation mechanism of nickel and cobalt, which was same to our conclusion. [26-27]

Another way was used to further verify the nucleation type of nickel deposition. The rising current should have a good linear relationship with $t^{2/3}$ for progressive nucleation model. Therefore, a plot of $t^{2/3}$ versus rising current was given in Fig.7.

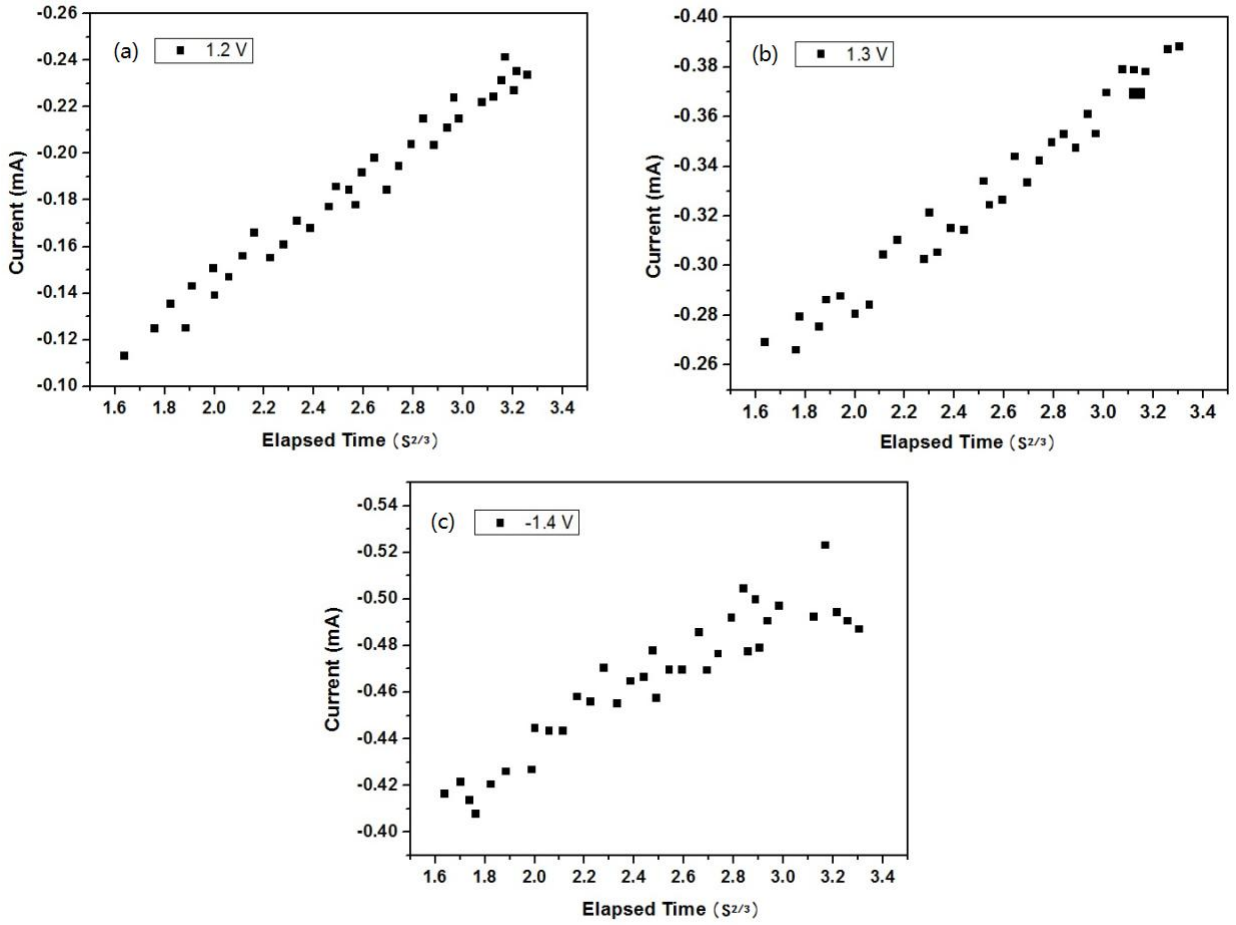

Figure 7. The relationship between rising current and $t^{2/3}$

The rising currents of nickel deposition with different voltages had linear relationship with $t^{2/3}$. Moreover, with the increase of voltages, the slope of lines increased. Larger slope indicated increase of nucleation sites. Consequently, it could draw the conclusion that reduction of nickel on the glassy carbon was a three dimensional progressive nucleation mechanism with electrochemical controlling.

3.3 Surface morphology of nickel deposition

In order to reduce the effects of other additives on nickel electrodeposition process, nickel films were prepared without adding complexing agents, brightener, and so on. From Fig.8, it was conspicuous that nickel films were densely covered with bulk structures.

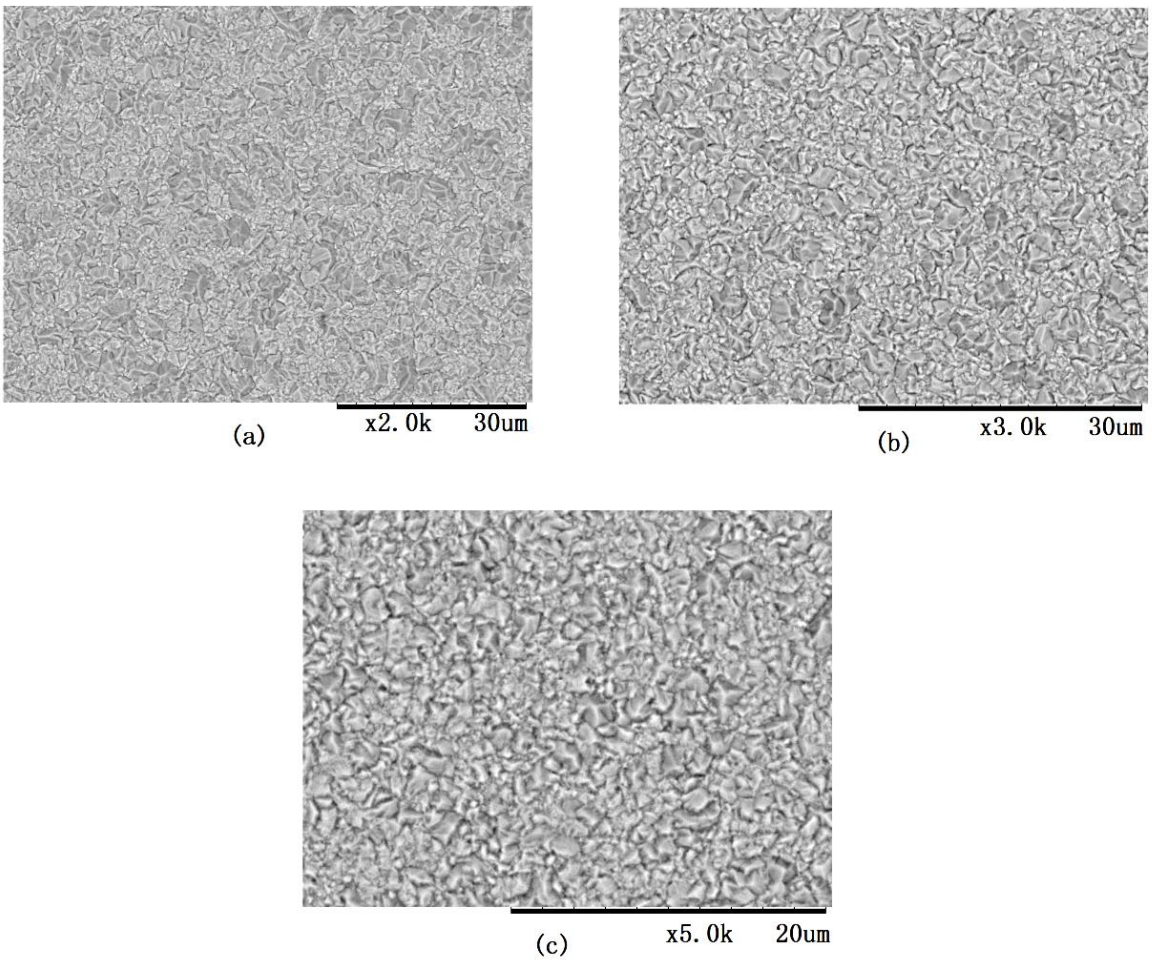

Figure 8. SEM images of nickel films prepared at -1.2 V_{SCE}

4. CONCLUSION

Nickel based alloy films have been becoming the hot spot of functional films, which were studied extensively. However, basic electrodeposition mechanism of nickel was seldom reported in detail. In the paper, nickel films were obtained on glassy carbon electrode to research nickel electrodeposition process by cyclic voltammetry, chronoamperometry and polarization curves. According to the results, no nickel deposition could be obtained when the voltage was lower than -0.2 V_{SCE}. Though nickel deposition could be obtained at the position with -0.6 V_{SCE}, hydrogen evolution was dominated. However, cathode current and deposition mass of nickel increased extremely when the voltage was more negative than -1.0 $V_{SCE.}$ Higher sweeping voltage would lead to stronger cathodic polarization process and more deposition mass. The data received from chronoamperometry curves in the form $(i/i_{max})^2$ against (t/t_{max}) were compared to the theoretical nucleation model to determine the nucleation type. It deduced that nickel electrodeposition on the glassy carbon indicated a kind of three dimensional progressive nucleation mechanism.

ACKNOWLEDGEMENT
This paper is supported by National Natural Science Foundation (No.51502278) & (No. 51471156).

References

1. B.J. Han, Y. Yang, L. Fang, G.H. Peng and C.B. Yang, *Int. J. Electrochem. Sci.*, 11 (2016) 9206.
2. E.P.S. Schmitz, S.P. Quinaia and J.R. Garcia, *Int. J. Electrochem. Sci.*, 11 (2016) 983.
3. R. Hu, Y.Y. Su and H.D. Liu, *J. Alloys Compd.*, 658 (2016) 555.
4. Y.Gao, J.H. Wang and J. Yuan, *Appl. Surf. Sci.*, 364 (2006) 740.
5. S. Mohajeri, A. Dolati and M. Ghorbani, *Surf. Coat. Technol.*, 262 (2015) 173.
6. P.A. Shaikh, R.C. Kambale, A.V. Rao and Y.D. Kolekar, *J. Alloys Compd.*, 492 (2010) 590.
7. C.D.M. Campos, A. Flacker, S.A. Moshkalev and E.G.O. Nobrega, *Thin Solid Film.*, 520 (2012) 4871.
8. X.M. Sun, Q.Yuan, D.M. Fang and H.X. Zhang, *Sens. Actuators. A.*, 188 (2012) 190.
9. J. Vilana, M. Lorenzo and E. Gomez, *Mater. Lett.*, 159 (2015) 154.
10. J.V. Arenas, I.R. Ibarra and R.H. Lara, *Ref. Mod. Mater. Sci. Mater. Eng.*, 3 (2017) 86.
11. F.F. Xia, J.Y. Tian and W.C. Wang, *Ceram. Int.*, 42 (2016) 13268.
12. N.P. Wasekar, S.M. Latha and M. Ramakrishna, *Mater. Des.*, 112 (2016) 140.
13. S. A. Ataie and A. Zakeri, *J. Alloys Compd.*, 674 (2016) 315.
14. J. Vilana, E. Gomez and E. Valles, *Appl. Surf. Sci.*, 360 (2016) 816.
15. T. Sahin, H. Kockar and M. Alper, *J. Magn. Magn. Mater.*, 373 (2015) 128.
16. Y.D. Yu, X.X.Zhao and M.G. Li, *Surf.Eng.*, 29 (2013) 743.
17. Y.D. Yu, Y. Cao and M.G. Li, *Mater.Res.Innovations.*, 18 (2014) 314.
18. Q.H. Lu, R. Huang, L.S. Wang and Z.G. Wu, *J. Magn. Magn. Mater.*, 394 (2015) 253.
19. Y.D. Yu, Z.L. Song, *Mater.Res.Innovations.*, 20 (2016) 280.
20. A. Krause, M. Uhlemann and A. Gebert, *Electrochimi. Acta*., 49 (2004) 4127.
21. M. Ebadi, W.J. Basirun and Y. Alias, *Mater. Charact*., 66 (2012) 46.
22. L.L. Tian, J.C. Xu and C.W. Qiang, *Appl. Surf. Sci*., 257 (2011) 4689.
23. J.A. Koza, M. Uhlemann and A. Gebert, *J. Electroanal. Chem*., 617 (2008) 194.
24. S. Topolovec, H. Krenn and R. Wurschum, *J. Magn. Magn. Mater*., 397 (2016) 96.
25. M. Ebadi, W. J. Basirun and Y. Alias, *Metall. Mater. Trans. A.*, 42 (2011) 2402.
26. Y.D. Yu, Z.L. Song and H.L. Ge, *Int. J. Electrochem. Sci*., 10 (2015) 4812.
27. M. Ebadi, W.J. Basirunn and Y. alias, *Metall. Mater. Trans. A*., 42A (2011) 2402.